Detection of Static Rotor Eccentricity in Permanent Magnet Synchronous Drives using Field Reconstruction Method

Amir Khoobroo, *Student member IEEE*
Renewable Energy and Vehicular Technology Lab
University of Texas at Arlington
#130, Nedderman Hall, 416, S. Yates St.,
Arlington, TX, USA, 76019
Email: amir.khoobroo@mavs.uta.edu

Babak Fahimi, *Senior Member IEEE*
Renewable Energy and Vehicular Technology Lab
University of Texas at Arlington
#130, Nedderman Hall, 416, S. Yates St.,
Arlington, TX, USA, 76019
Email: fahimi@uta.edu

***Abstract*— Permanent magnet synchronous motor (PMSM) drives are increasingly considered in vehicular applications due to relatively high power density, negligible rotor losses, high efficiency, ease of control, and maintenance. In this paper a new method of fault detection and treatment for 5-phase PMSM under static rotor eccentricity has been introduced. As the optimum performance is of great importance in vehicular applications the excitation of stator phases has been modified to attain the maximum output torque per input phase current in the event of rotor eccentricity. Field reconstruction method has been used in conjunction with optimization methods to detect the fault and find the appropriate excitation.**

I. INTRODUCTION

Fault tolerance has become a design criterion for adjustable speed motor drives (ASMD) used especially in high impact applications. A fault tolerant ASMD is expected to continue its intended function in the event of a failure by squeezing the maximum power available compliment of the remaining components. There are different types of fault that may occur in the ASMD. In case of a PMSM drive, besides the regular monitoring of the current and voltage levels, other quantities such as the airgap length should be monitored to avoid further damage due to the collision of rotor and stator caused by eccentricity (i.e. unbalanced magnetic pull). In addition, the saturation of the stator core due to eccentricity reduces the productivity of the machine in terms of output power and torque. As the continuity of the service is of great importance, the next step would be to calculate the best excitation possible for the stator phases of the machine to harvest maximum torque.

A vast amount of the research has been done on development of health monitoring methods [1- 9]. Most of these researches focus only on detection of the fault and do not address the treatment of the machine in the aftermath of the fault. Furthermore, most of the methods just apply to the specific faults on the stator windings and are not applicable to the other types of the fault.

Field reconstruction method (FRM) is a recent method that improves the computational time necessary to determine the distribution of magnetic field components. FRM is an alternative to Finite Element Analysis (FEA) with comparable accuracy, but with significantly shorter computational time. The literature and the applications of the method have been addressed [10-16]. This method uses the field created by a single slot on the stator, along with the field generated by the permanent magnets (windings) on the rotor of the AC machine, to find the field distribution and electromagnetic force components.

In this paper the field reconstruction method (FRM) has been used to detect static rotor eccentricity in an adjustable speed PMSM drive. The FRM has been used to estimate the flux passing through each stator tooth for the fault detection purpose. In addition FRM has been used in conjunction with optimization methods to find the optimal stator currents which would be used for post fault operation.

II. FIELD RECONSTRUCTION

In order to verify the field reconstruction method a model has been developed for the PMSM using MAGNET from Infolytica©. A 10 hp, 5-phase, 6-pole, 30 slot surface mounted permanent magnet synchronous machine is used in this study. The 3D model of the machine is shown in Fig. 1. In this modeling the following assumptions are made:

- No deformations in the permanent magnets or stator teeth due to internal forces.
- Concentrated stator windings.
- No end coil effect.

U.S. Government work not protected by U.S. copyright

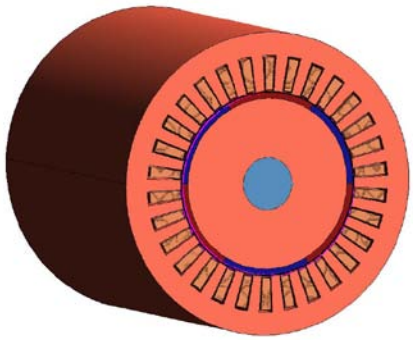

Figure 1: 3D view of the PMSM model

It can be shown that the magnetic field components need to be known in order to calculate the torque. The FEA methods are conventional tools to calculate the magnetic field components. However, they are time consuming and, hence, inadequate for iterative procedures such as those used in optimization processes. FRM has been used to analyze the magnetic field components. It is shown in [12] that for an unsaturated PMSM the magnetization curve can be considered to be linear and, as such, the superposition rule is applied to the field components as follows:

$$B_t = B_{tpm} + B_{ts} \quad (1)$$

$$B_n = B_{npm} + B_{ns} \quad (2)$$

Where, B_{npm}, B_{tpm} B_{ns} and B_{ts} denote the normal and tangential field components due to the permanent magnets and stator currents respectively. The resultant magnetic field created by the stator windings is the sum of the field created by each individual stator slot current. The normal and tangential field components due to the stator currents can be written as:

$$B_{ns} = \sum_{k=1}^{L} B_{nsk} \quad (3)$$

$$B_{ts} = \sum_{k=1}^{L} B_{tsk} \quad (4)$$

To evaluate (3) and (4) the local flux densities created by the current in the k^{th} slot is expressed as follows:

$$B_{tsk}(\phi_s) = I \,.\, f_1(\phi_s) \quad (5)$$

$$B_{nsk}(\phi_s) = I \,.\, f_2(\phi_s) \quad (6)$$

Where f_1 and f_2 associated with the geometry. A single magnetostatic FEA is needed to find these basis functions. Having these basis functions for a typical slot say 1^{st} carrying current I_0 (5) and (6) can be rewritten as:

$$B_{tsk} = (I/I_0)B_{ts0}(\phi - k\gamma) \quad (7)$$

$$B_{nsk} = (I/I_0)B_{ns0}(\phi - k\gamma) \quad (8)$$

Therefore by performing a single off-line FEA for a single slot contribution of the stator to the rotating field components can be calculated for any normal working condition. In the second step, permanent magnet contribution to the field, over one pole pitch, is computed using an FEA analysis for the unexcited stator condition. Having these two components the magnetic field components can be obtained in the middle of the airgap. The field reconstruction flowchart is shown in Fig. 2. In order to verify the accuracy of this method the tangential and normal components of the magnetic field in the middle of the airgap obtained from FRM have been compared to those from FEA. Figures 3 and 4 depict the accuracy of field reconstruction method. The accuracy of the method can be improved further by increasing the resolution of the basis functions.

There are a variety of ways to calculate the electro-mechanical force in electrical machines [17]. Among the existing options Maxwell Stress Tensor (MST) method is utilized here. According to MST the force components densities in the airgap can be calculated using the following formulae:

$$f_t = B_n B_t / \mu_0 \quad (9)$$

$$f_n = (B_n^2 - B_t^2)/2\mu_0 \quad (10)$$

In which B_n and B_t are normal and tangential components of the magnetic flux density. Thus, the force components would be as follows:

$$F_t = \oint_{\Gamma} \vec{f}_t . dl \quad (11)$$

$$F_n = \int_0^{2\pi} f_n r d\phi \quad (12)$$

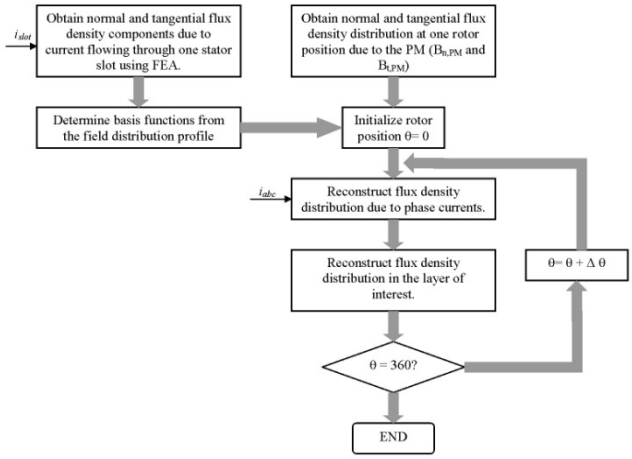

Figure 2: Field reconstruction method flowchart

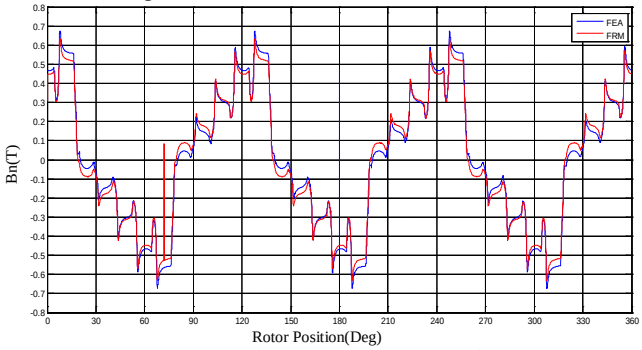

Figure 3: Comparison of FEA and FRM, Normal field component

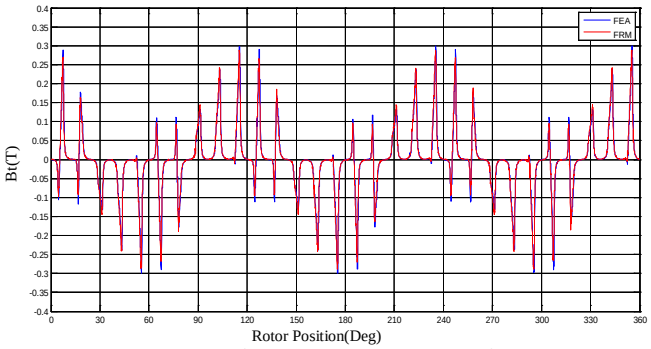

Figure 4: Comparison of FEA and FRM, Tangential field component

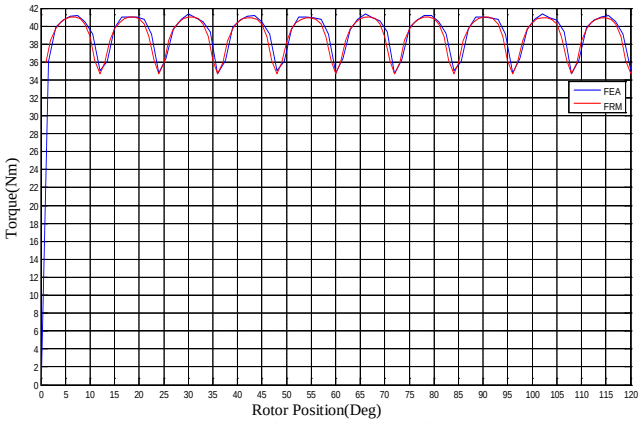

Figure 5: Comparison of torque obtained from FEA and FRM

Where, *r* is the integration contour. It is obvious that for torque calculations magnetic field components should be known. The MST method is quite effective provided that the FEA solutions are precise. The torque comparison for FEA and FRM is shown in Fig. 5. In the following sections the FRM method is used for detection purposes to estimate the flux passing through each stator tooth. Also, this method has been combined with the MATLAB optimization tool box to achieve the optimal waveforms in case one or more of the stator phases are disengaged.

III. MAGNETIC FLUX CALCULATION

In this section, first the method used for calculating the flux flowing through each stator tooth will be derived and then used to calculate the flux linking each stator phase.

A. Stator teeth fluxes

In the first step, using the field components in the middle of the airgap, the flux passing through the stator tooth would be calculated. The magnetic field distribution in the first quadrant of the PMSM model is shown in Fig. 6. According to this figure a dominant majority of the flux lines that exist in the airgap would enter the stator tooth from the top surface. So, the flux in each stator tooth can be calculated using the magnetic field components in the airgap. There would be a slight error in this calculation because of the leakage flux (i.e. some flux lines would enter the stator tooth from the tooth side surfaces instead of top surface). These flux lines are not accounted for, in the calculation and therefore result in error.

The flux density components are projected on the axis passing the middle of each tooth. This can be done using the following equation:

$$B_{proj}(j) = \sum_{i=1}^{K} \{B_{n,i}\cos(\phi_i - \theta_j) - B_{t,i}\sin(\phi_i - \theta_j)\} \qquad (13)$$

Where ϕ and θ are the position of the field components in the airgap and the position of the projection axis in the model respectively. The indices $i = 1...K$ and $j = 1...L$ refer to the number of field component solutions in the airgap covering one stator tooth and the respective stator teeth, respectively. Based upon normal field components, the flux in the airgap, which is almost equal to the flux in the stator tooth, can be calculated as:

$$\Phi = \iint_S \vec{B}_{proj} . d\vec{S} \qquad (14)$$

The above integration is performed on the surface which is concentric to the rotor surface and passes through the stator teeth as shown in Fig.7.

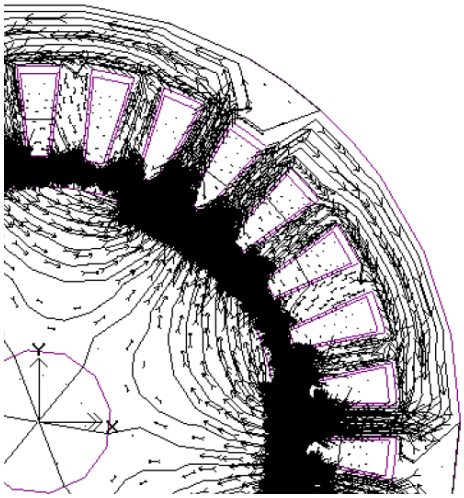
Figure 6: Magnetic Flux distribution in the machine

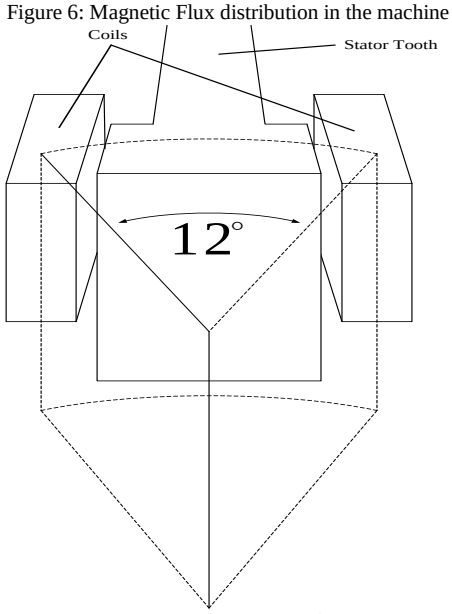

Figure 7: Integration surface

B. 5 phase flux linkages

In order to calculate the stator phase flux linkage, the flux is calculated for one pole and then multiplied by the number of pole pairs. Fig. 8 depicts the flux corresponding to the first pole which passes through the A1-A2 frame (linking A1-A2). The flux linkage of this winding is as follows:

$$\lambda_{A1-A2} = N(\Phi_2 + \Phi_3 + \Phi_4 + \Phi_5 + \Phi_6) \quad (15)$$

Phase A flux linkage is as follows:

$$\lambda_A = 3N(\Phi_2 + \Phi_3 + \Phi_4 + \Phi_5 + \Phi_6) \quad (16)$$

Where, N represents the number of conductors in each coil. This equation could be generalized into the following form for a machine with *q* stator tooth per pole and 2P magnetic poles (P represents the number of magnetic pole pairs):

$$\lambda_A = PN * \sum_{k=1}^{q} \Phi_k \quad (17)$$

The same analysis can be carried out for phases B, C, D and E. Fig. 9 depicts flux passing through stator teeth 1 to 5 calculated using the observer compared to the FEA. Fig. 10 depicts phase "A" flux linkage calculated using the proposed method, compared to that of the FEA.

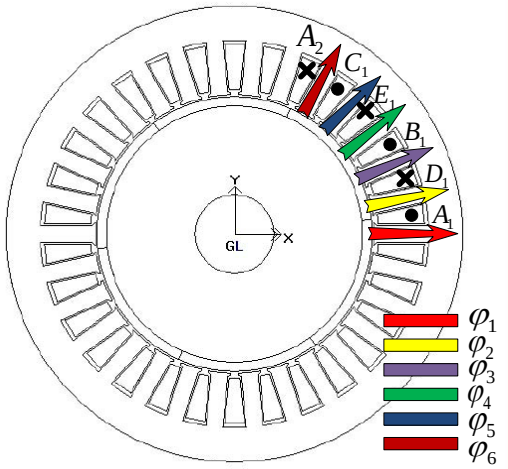

Figure 8: Flux assignment to stator teeth

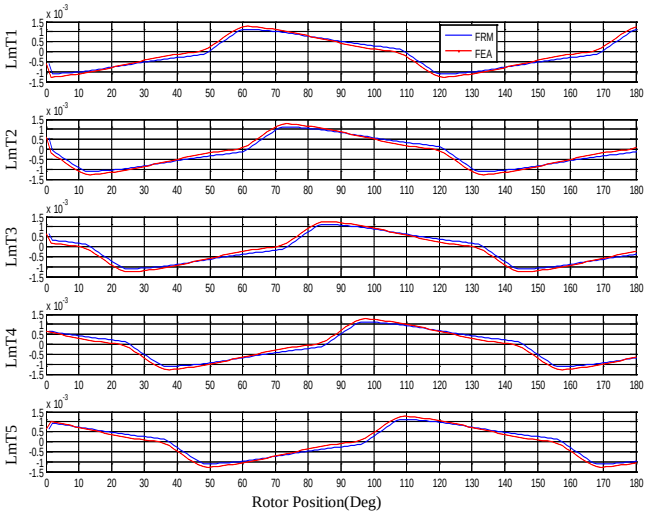

Figure 9: Comparison of stator teeth flux obtained from FEA and FRM

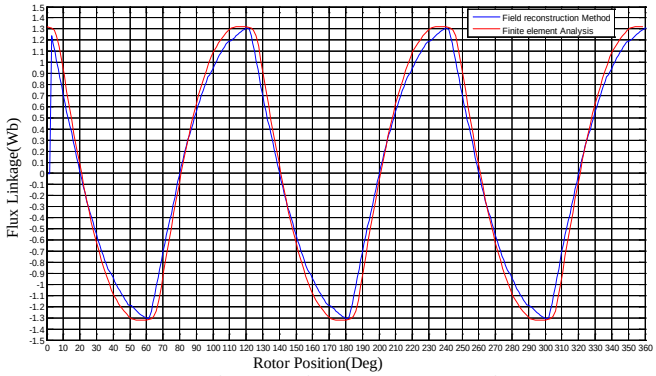

Figure 10: Comparison of Phase A flux linkage obtained from FEA and FRM

It can be seen that, while much faster, the flux observer is quite accurate compared to FEA.

IV. STATIC ROTOR ECCENTRICITY DETECTION

In case of eccentricity as the rotor is closer to a set of windings, the balance no longer exists in the electrical quantities, so for the same amount of current applied as of the healthy case some of the stator teeth would have higher levels of magnetic flux due to the proxomity to the permanent magnets. In this analysis the static eccentricity of the rotor is assumed to be %30 as shown in Fig.11.

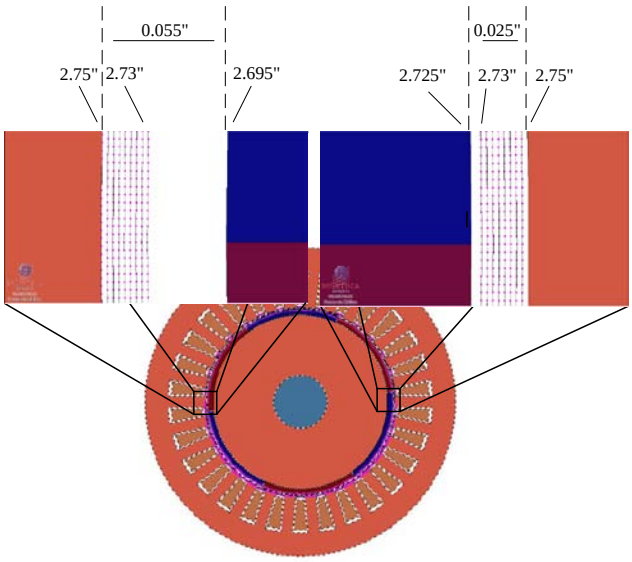

Figure 11: Eccentric 5-phase PMSM

Fig. 12 depicts the comparison of the magnetic flux distribution in the machine in case of a healthy machine and the one with an eccentric rotor. It can be seen that the peak of magnetic flux is higher in case of eccentric rotor. Also, in case of eccentric rotor the distribution of the magnetic flux around the airgap is no longer uniform. This signature can be used to determine the eccentricity of the rotor. In case of an eccentric rotor the magnetic flux can be written as:

$$\Phi_j(\theta_e) = \Phi_{PM,j}(\theta_e) + \sum_{j=1}^{5} i_j(\theta_e - j\frac{2\pi}{5}).\Phi_j(\phi_S - j\frac{2\pi}{5}) \Rightarrow \int_0^{2\pi} \Phi_j(\theta_e) d\theta_e \neq 0 \quad (18)$$

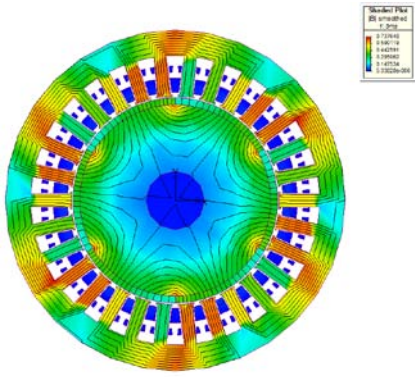

(a)

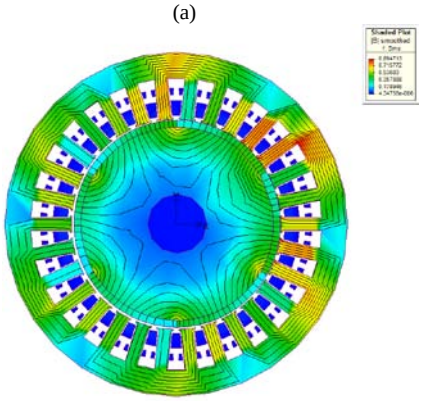

(b)

Figure 12: Comparison of magnetic flux distribution (a) healthy machine (b) eccentric rotor

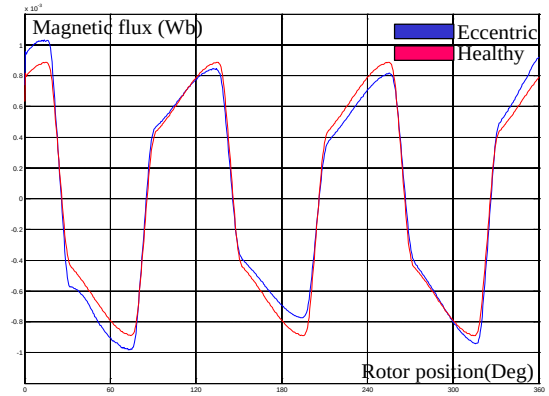

(a)

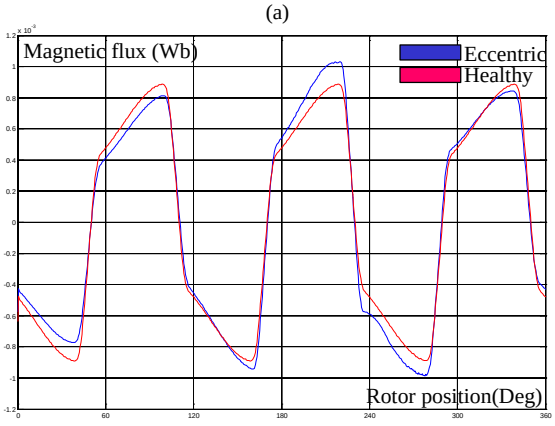

(b)

Figure 13: Comparison of magnetic flux distribution (a) tooth #3 (b) tooth #20

The flux passing each stator tooth is measured using the FRM module and compared with the flux for the healthy case and the unbalance of the flux shows the eccentricity of the rotor. It should be mentioned that in case of an eccentric rotor there is no deformity in the magnetic flux wavefrom as observed in case of PM demagnetization and the difference is in the magitude of the flux. Fig. 13 depicts the flux passing stator teeth in case of eccentric rotor compared with the healthy machine. In this case the static eccentricity of 30% has been considered for the rotor.

V. FAULT TREATMENT

Depending on the service continuity strategy, various scenarios can be deployed after the fault is detected. In case, the service can be provided by another module the machine could be stopped and the eccentricity caould be fixed. In case of an emergency application in which service discontinuity is not possible the stator applied currents can be modified in a way the maximum possible average torque could be squeezed out of the machine shaft. Of course the presence of the harmonics in the current would result in extra torque pulsations. For this purpose the field reconstruction method would be used in conjunction with the optimization methods to attain the optimal current waveforms. The fault detection and treatment scheme is shown in Fig. 14.

Fig. 15 depicts the output mechanical torque of the machine for static rotor eccentricity fault in case sinusoidal currents are applied to stator phases. It is shown that the average torque has decreased almost 25% as a result of the eccentricity. Also torque ripple has been increased almost 30% compared with the healthy operation condition. Using the optimization methods the optimal waveforms are determined in case, static eccentricity occurs. The Matlab optimization toolbox is linked to the FRM code. For each rotor position, the optimization code calculates a set of currents based on the optimization criteria. These currents are used to calculate the magnetic field components in the machine. Then, using the magnetic field components the torque is calculated using (11). In case the calculated torque complies with the target values, the currents would be stored and a new rotor position would be considered. Fig. 16 depicts the optimal stator phase currents and the output torque of the machine.

The optimization criteria can be chosen to achieve the following cases regarding the target application:

- Maximum average torque
- Maximum average and Minimum torque ripple
- Minimum torque ripple

Here, the optimization process is targeted towards the maximum average torque. It can be seen that the average torque is about 3% less than that of the healthy with sinusoidal stator currents. The torque ripple is increased as expected. Different optimization scenarios can be considered and the optimal currents for each case can be achieved and stored in look up tables in the control unit. Based on the application, the appropriate currents can be applied to stator phases in case the fault is detected.

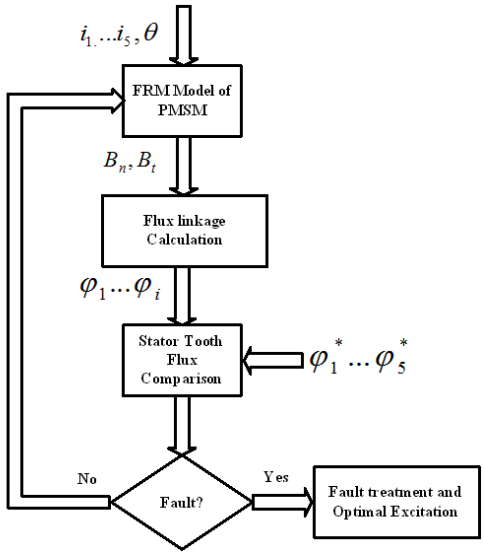

Figure 14: Fault detection alghorithm

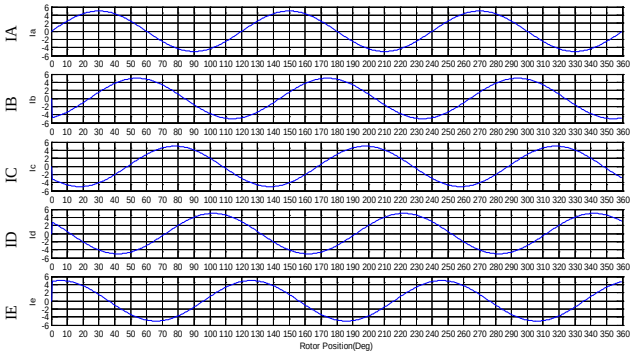

Rotor Position (Deg)

(a)

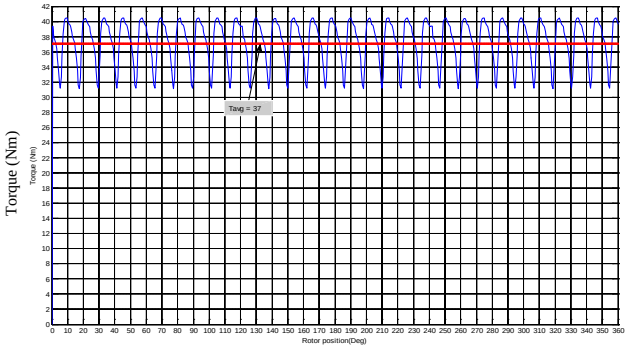

Rotor Position (Deg)

(b)

Figure 15: Torque Analysis. (a) Sinusoidal stator currents, (b) Eccentric rotor

VI. CONCLUSION

Field reconstruction method as a powerful magnetic field analysis tool can be used to detect the faults in the PMSM. Demagnetization of the magnets in PMSM is one of the major issues with this type of the machine especially at higher power ratings. It can occur due to high temperatures resulting from poor ventilation or excessive short circuit currents and of course the aging of the magnets. In this paper a new way of demagnetization fault detection has been presented. The flux linkages of the stator phases are calculated using the FRM and used to monitor the faults. FRM can be linked to the optimization tools to achieve the optimal currents which yield maximum average torque and/ or minimum torque ripple. After detecting the fault the optimal currents could be applied to improve output torque characteristic of the machine.

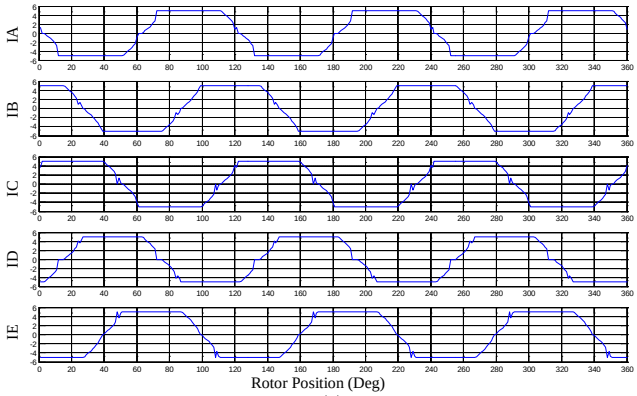

(a)

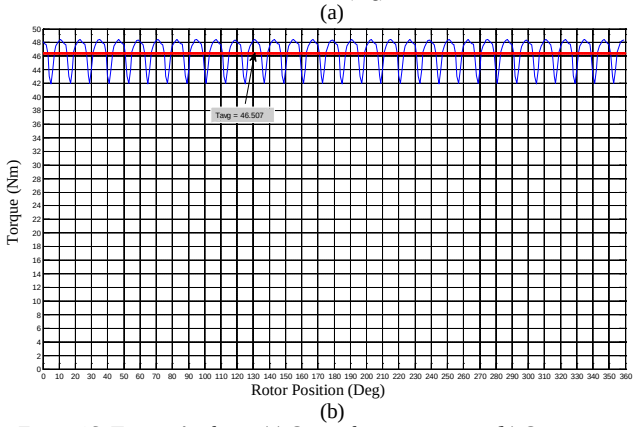

(b)

Figure 16: Torque Analysis. (a) Optimal stator currents, (b) Output torque, static rotor eccentricity

REFERENCES

[1] J. W. Bennett, B. C. Mecrow, A. G. Jack, D. J. Atkinson, S. Sheldon, B. Cooper, G. Mason, C. Sewell, D. Cudley, "A prototype electrical actuator for aircraft flaps and slats", *IEEE Int. Conf. on Electrical machines and Drives*, pp. 41 - 47 , 2005.

[2] N. Ertugrul, W. Soong, G. Dostal, D. Saxon, "Fault tolerant motor drive system with redundancy for critical applications", *IEEE Power Electronics Specialists Conf.*, pp. 1457 - 1462, 2002.

[3] G. J. Atkinson, B. C. Mecrow, A. G. Jack, D. J. Atkinson, P. Sangha, M. Benarous, "The design of fault tolerant machines for aerospace applications", *IEEE Int. Conf. on Electric machines and Drives*, pp. 1863 - 1869, 2005.

[4] Z. Jingwei, N. Ertugrul, L. S. Wen, "Detection and Remediation of Switch Faults on a Fault Tolerant Permanent Magnet Motor Drive with Redundancy", *IEEE ICIEA Conf.* pp. 96 - 101,2007.

[5] B. C. Mecrow, A. G. Jack, J. A. Haylock, J. Coles, "Fault tolerant permanent magnet machine drives", *IEEE Int. Conf. on Electrical machines and Drives*, pp. 433 - 437, 1995.

[6] C. Opera, C. Martis, "Fault Tolerant Permanent Magnet Synchronous Machine for electric power steering systems", *Int. Sym. on Power Electronics, Electrical Drives, Automation and Motion (SPEEDAM)*, PP. 256 – 261, 2008.

[7] B. M. Ebrahimi, J. Faiz, M.J. Roshtkhari, " Static-, Dynamic-, and Mixed-Eccentricity fault diagnoses in permanent-magnet synchronous motors", *IEEE Trans. on Ind. Electron.*, Vol. 56, No. 11, pp. 4727–4739, 2009.

[8] J. Rosero, L. Romeral, J. A. Ortega, J.C. Urresty, "Demagnetization fault detection by means of Hilbert Huang transform of the stator

current decomposition in PMSM", *Int. Sym. on Industrial Electronics (ISIE)*, pp. 172 – 177, 2008.

[9] J. A. Rosero, J. Cusido, A. Garcia, J. A. Ortega, L. Romeral, "Study on the Permanent Magnet Demagnetization Fault in Permanent Magnet Synchronous Machines", *IEEE conf. on Industrial Electronics*, pp. 879 – 884, 2006.

[10] A. Khoobroo, B. Fahimi, S. Pekarek, **"**A New field reconstruction method for permanent magnet synchronous machines"**,** *Int. Conf. on Ind. Electron.*, pp. 2009 – 2013, 2008.

[11] A. Khoobroo, B. Fahimi, "A new method of fault detection and treatment in five phase permanent magnet synchronous machine using field reconstruction method", *IEEE Int. Conf. on Electric machines and Drives*, pp. 682 – 688, 2009.

[12] W. Zhu, B. Fahimi, S. Pekarek, **"**A field reconstruction method for optimal excitation of permanent magnet synchronous machines"**,** *IEEE Trans. on Energy Conversion*, vol. 21, no.2, pp. 305 – 313, June 2006.

[13] B. Fahimi, "Qualitative approach to electromechanical energy conversion: Reinventing the art of design in adjustable speed drives", *Int. Conf. on Electrical machines and Systems*, pp. 432 – 439, Oct 2007.

[14] W. Zhu, B. Fahimi, S. Pekarek, **"**Optimal excitation of permanent magnet synchronous machines via direct computation of electromagnetic force components", *IEEE Int. Conf. on Electrical machines and Drives*, pp. 918 - 925 , May 2005.

[15] A. Kioumarsi, M. Moallem, B. Fahimi, **"**Mitigation of Torque Ripple in Interior Permanent Magnet Motors by Optimal Shape Design", *IEEE Trans. on Magnetics*, vol. 42, no.11, pp. 3706 – 3711, Nov 2006.

[16] W. Jiang, M. Moallem, B. Fahimi, S. Pekarek, **"**Qualitative Investigation of Force Density Components in Electromechanical Energy Conversion Process", *IEEE Conf. on Ind. Electron.*, pp.1113-1118, Nov. 2006.

[17] A. Belahcen, "Overview of the calculation methods for forces in magnetized iron cores of electrical machines," *presented at the Seminar on Modeling and Simulation of Multi-Technological Machine Systems*, vol. 29, pp. 41–47, Nov. 1999.